

# Integrative omics analysis identifies subtypes with therapeutic implications in lung adenocarcinoma harboring KEAP1/NFE2L2

**Xiaodong Yang**

Shanghai Pulmonary Hospital

**Ming Li**

Zhongshan Hospital

**Zhencong Chen**

Zhongshan Hospital

**Liang Guo**

Shanghai Pulmonary Hospital

**Bo Jin**

Zhangqiu District People's Hospital

**Yiwei Huang**

Zhongshan Hospital

**Qun Wang**

Zhongshan Hospital

**Liang Wu**

Shanghai Pulmonary Hospital

**Cheng Zhan** (✉ [czhan10@fudan.edu.cn](mailto:czhan10@fudan.edu.cn))

Zhongshan Hospital

---

## Research Article

**Keywords:** lung adenocarcinoma, KEAP1, mutation, NFE2L2

**Posted Date:** March 3rd, 2021

**DOI:** <https://doi.org/10.21203/rs.3.rs-182066/v1>

**License:**   This work is licensed under a Creative Commons Attribution 4.0 International License.

[Read Full License](#)

---

# Abstract

**Backgrounds:** Lung adenocarcinoma is one of the most common malignant tumors, in which *KEAP1-NFE2L2* pathway is altered frequently. The biological features and intrinsic heterogeneities of *KEAP1/NFE2L2*-mutant lung adenocarcinoma remain unclear.

**Methods:** Multiplatform data from The Cancer Genome Atlas (TCGA) were adopted to identify two subtypes of lung adenocarcinoma harboring *KEAP1/NFE2L2* mutations.

Bioinformatics analyses, regarding immune microenvironment, methylation level and mutational signature, were performed to characterize intrinsic heterogeneities. Meanwhile, initial results were also validated by using common lung adenocarcinoma cell lines, which revealed consistent features of *KEAP1/NFE2L2*-mutant subtypes. Furthermore, cell line samples were adopted for drug sensitivity screening based on public datasets.

**Results:** Two mutant subtypes (P1 and P2) of patients were identified in TCGA. P2 patients had significantly heavier smoking levels and worse survival compared with P1 patients. The P2 subset was characterized by active immune microenvironment and more smoking-induced genomic alterations, including methylation and somatic mutations. Validations of the corresponding features in mutant cell lines were achieved to some degrees. Several compounds which were sensitive to mutant subtype of lung adenocarcinoma were identified, such as inhibitors of *PI3K/Akt* and *IGF1R* signaling pathways.

**Conclusions:** *KEAP1/NFE2L2* mutant lung adenocarcinoma showed potential heterogeneities. The intrinsic heterogeneities of *KEAP1/NFE2L2* were associated with immune microenvironment and smoking-related genomic aberrations.

## Introduction

Lung cancer is the leading cause of cancer-associated morbidity and mortality worldwide, among which lung adenocarcinoma accounts for the highest proportion with increasing incidence [1–4]. Previous studies promoted a paradigm shift regarding classifying lung tumors based on the significant genomic alterations for therapeutic targets, such as epidermal growth factor receptor (*EGFR*) and anaplastic lymphoma kinase (*ALK*) [5–7]. The Kelch-like ECH-associated protein 1 (*KEAP1*) and the nuclear factor erythroid-2-related factor 2 (*NFE2L2*) mutations were found in more than 20% patients with non-small cell lung cancer, which represented one of the most important genomic subtypes [8, 9]. Moreover, the genomic alterations of *KEAP1* or *NFE2L2* were reported to play crucial roles in lung adenocarcinoma [10–12].

Abnormal regulations of reactive oxygen species contribute to the occurrence and development of malignancies [13]. The *KEAP1* and *NFE2L2* are the two main components in the stress response pathways. *KEAP1* mediates the degradation of *NFE2L2* to act as an adaptor protein of the Cullin 3 (*CUL3*) E3 ubiquitin ligase so as to maintain the redox homeostasis. In the presence of oxidative stress, the inactivation of *KEAP1* results in the release, accumulation and nucleus translocation of *NFE2L2* to

counteract the damage [14, 15]. Therefore, the *KEAP1/NFE2L2* mutations, representing the dysfunctional activations of the stress response pathway, have been found in many common malignant tumors, including lung adenocarcinoma [16–18]. Nevertheless, the biological features and clinical implications of *KEAP1/NFE2L2* mutations remain elusive and contradictory. Rizvi et al revealed potential associations between the response of immune checkpoint inhibitors and *KEAP1*-mutant non-small cell lung cancer. On the contrary, Hellyer et al suggested that *KEAP1/NFE2L2* mutations might represent a mechanism of intrinsic resistance to *EGFR*-tyrosine kinase inhibitor therapy [19]. Chemoresistance was also reported to be associated with *KEAP1/NFE2L2* mutations [20, 21].

In our study, multiplatform data from The Cancer Genome Atlas (TCGA) was adopted to identify two subtypes of lung adenocarcinoma harboring *KEAP1/NFE2L2* mutations. Bioinformatics analyses regarding immune microenvironment and methylation level were performed to characterize potential mutant subgroups. The initial results were also validated by using common lung adenocarcinoma cell lines, which revealed consistent features of *KEAP1/NFE2L2*-mutant subtypes. Furthermore, cell line samples were adopted for drug sensitivity screening based on public datasets. Potential drugs which were sensitive to each mutant subtype of lung adenocarcinoma were explored and identified.

## Methods

### Patient cohort and cell lines data

Level 3 RNA sequencing data, DNA methylation data (Illumina Infinium HumanMethylation 450K BeadChip), miRNA expression data and clinical information of patients with lung adenocarcinoma were downloaded from TCGA (<https://portal.gdc.cancer.gov/>). Somatic mutation data were selected based on previous studies by comprehensive analyses accounting for variance and batch effects [22]. Copy number variations (CNV) were estimated using the GISTIC2 method from the University of California Santa Cruz Xena website (<https://xena.ucsc.edu>). Patients with *KEAP1/NFE2L2* mutations were selected as the main study cohort. Patients with missing data types were excluded.

RNA sequencing data, miRNA expression levels, copy number values and gene mutation status of common lung adenocarcinoma cell lines were downloaded from the Cancer Cell Line Encyclopedia (CCLE, <https://portals.broadinstitute.org/ccle>). Also, DNA methylation levels (Illumina Infinium HumanMethylation 450K BeadChip) of selected cancer cell lines were acquired from the Gene Expression Omnibus (GEO, (<https://www.ncbi.nlm.nih.gov/geo>) (GSE68379). The drug sensitivity data of selected cancer cell lines were obtained from the Genomics of Drug Sensitivity in Cancer (GDSC, <https://www.cancerrxgene.org/>). Histological information of each cell line was confirmed based on GDSC, CCLE and Cellosaurus database [23, 24]. Cell lines with unknown data types were removed. Similarly, lung adenocarcinoma cell lines with *KEAP1/NFE2L2* mutations were identified by following the above rules.

### Data processing and clustering

For the DNA methylation data, probes in sex chromosomes or overlapping single nucleotide polymorphisms were removed. Cross-reactive probes were also excluded according to Chen et al [25]. The frequencies of six base substitutions (C > A, C > G, C > T, T > A, T > C, and T > G) were calculated. For some datasets, features or probes with more than 20% missing values were deleted. The k-nearest neighbor algorithm was adopted to impute the remaining missing data.

All five data types (RNA sequencing, DNA methylation, miRNA level, copy number and base substitution) were integrated using the similar network fusion (SNF) method for lung adenocarcinoma patients and cell lines. The SNF method fused all five datasets into one by creating a similarity matrix for each data type. A non-linear method based on the theory of message-passing was adopted to iteratively update and converge datasets. Afterwards, consensus clustering was performed to identify distinct *KEAP1/NFE2L2* mutated subgroups of lung adenocarcinoma patients and cell lines [26].

### **Bioinformatics analyses to characterize *KEAP1/NFE2L2*-mutant subgroups**

Mutant subgroups were preliminarily characterized by subjecting clusters for both patients and cell lines to Gene Set Enrichment Analysis (GSEA) using Hallmark, Kyoto Encyclopedia of Genes and Genomes (KEGG), and Gene Ontology (GO) (MSigDB v7.0) gene sets [27]. Normalized enrichment score > 1, nominal *P*-value < 0.05, and false discovery rate *Q*-value < 0.25 were used as screening thresholds for GSEA. Moreover, we also explored potential concurrent mutations with *KEAP1/NFE2L2*-mutant subsets in lung adenocarcinoma patients.

The features of tumor microenvironment in *KEAP1/NFE2L2*-mutant lung adenocarcinoma were evaluated according to several previous studies. Saltz et al proposed a leukocyte fraction by estimating tumor-infiltrating leukocytes on hematoxylin and eosin stained slides using deep learning techniques [28]. We also used the “Estimation of STromal and Immune cells in MAlignant Tumours using Expression data (ESTIMATE)” method for the assessment of tumor microenvironment [29]. Li et al developed a public resource (Tumor IMMune Estimation Resource, TIMER) to study tumor-infiltrating immune cells by computational approaches based on RNA sequencing [30]. The levels of specific immune cell infiltration, like CD8 + T cell and macrophage, between mutant subgroups were also compared. Furthermore, we compared the number of immunogenic mutations and non-synonymous mutations per sample stratified by the *KEAP1/NFE2L2* mutant status.

The global methylation levels ( $\beta$  value) between *KEAP1/NFE2L2* mutant patient and cell line subsets were compared to investigate epigenomic alterations and potential clinical associations. Next, a list of smoking-related DNA methylation probes was obtained from a previous study conducted by Vaz et al. Vaz et al performed two repeated experiments with respect to chronic-cigarette-smoking-induced hypermethylated probes [31]. The union of all reported probes was considered and their levels stratified by the mutant subsets were compared. Somatic mutation status of *KEAP1/NFE2L2*-mutant patients was analyzed to extract mutational signatures using the SignatureAnalyzer [32]. Similarities were compared based on previously reported thirty mutational signatures in the Catalogue Of Somatic Mutations In

Cancer (COSMIC, <https://cancer.sanger.ac.uk/cosmic>) to identify the potential clinical associations and etiologies.

Cancer-associated drug sensitivity data of lung adenocarcinoma cell lines were also downloaded from two sub-datasets of GDSC. Drug samples that were tested in < 50% cell lines were excluded. The natural log value of the fitted half-maximal inhibitory concentration [LN(IC50)] of each drug was adopted to select cancer-associated drugs which were specifically sensitive to mutant subtypes (C1 and C2). The criteria for *KEAP1/NFE2L2*-mutant specific drugs were as follows:  $\text{LN(IC50)}_{\text{C1 or C2}} < \text{LN(IC50)}_{\text{C2 or C1}}$ ,  $P < 0.05$ ;  $\text{LN(IC50)}_{\text{C1 or C2}} < \text{LN(IC50)}_{\text{WT}}$ ,  $P < 0.05$ ; and  $\text{LN(IC50)}_{\text{C2 or C1}} \approx \text{LN(IC50)}_{\text{WT}}$ ,  $P > 0.05$ . However, only one C2-specific drug could be identified using the revised criteria:  $\text{LN(IC50)}_{\text{C2}} < \text{LN(IC50)}_{\text{C1}}$ ,  $P < 0.1$ ;  $\text{LN(IC50)}_{\text{C2}} < \text{LN(IC50)}_{\text{WT}}$ ,  $P < 0.1$ ; and  $\text{LN(IC50)}_{\text{C1}} \approx \text{LN(IC50)}_{\text{WT}}$ ,  $P > 0.1$ .

## Statistical analysis

All statistical analyses in this study were conducted using R version 3.6.1 (R Foundation for Statistical Computing, Vienna, Austria) and IBM SPSS Statistics 22.0 (IBM, Inc., NY, USA). Comparisons of immunological features and drug sensitivities were performed using the Kruskal-Wallis H test and Mann-Whitney U test. Baseline characteristics and co-mutations were compared by the chi-square test. Survival curves were estimated and compared following the Kaplan-Meier method and the log-rank test. A two-tailed *P*-value less than 0.05 was considered statistically significant.

## Results

### Identification of subtypes of *KEAP1/NFE2L2*-mutant lung adenocarcinoma

As previously stated in the Methods section, we integrated five data subtypes and clustered 89 *KEAP1/NFE2L2*-mutant lung adenocarcinoma patients into two subgroups (P1 and P2 groups, Fig. 1A). Similarly, two subtypes were identified in 20 lung adenocarcinoma cell lines harboring *KEAP1/NFE2L2*-mutations (C1 and C2 groups, Fig. 1C). Clustering with two classes in both patients and cell line samples showed the highest silhouette values (silhouette = 0.93 and 0.83, Fig. 1B and 1D).

### Clinicopathological differences of the *KEAP1/NFE2L2*-mutant subtypes

A significant difference was found in the smoking status of patients in P1, P2 and wild-type groups ( $P = 0.033$ , Table 1). The P2 group consisted of the highest proportions of current smokers and reformed smokers for  $\leq 15$  years, while P1 groups consisted of more reformed smokers  $\geq 15$  years (Table 1). No significant difference of pathological stage was found among patients with P1, P2 and *KEAP1/NFE2L2* wild-type lung adenocarcinoma ( $P = 0.233$ , Table 1). Mutant samples contained a significantly higher proportion of female patients ( $P = 0.003$ , Table 1). Survival analysis showed no significant difference in the overall survival between subgroups of *KEAP1/NFE2L2*-mutant and wild-type lung adenocarcinoma ( $P = 0.212$ , Fig. 2A). However, the P2-mutant subgroup was associated with a significantly worse survival than the P1 subgroup ( $P = 0.020$ , Fig. 2B).

Table 1

Baseline characteristics of wild type and *KEAP1/NFE2L2* mutant subgroups of lung adenocarcinoma samples in TCGA

	Wild type	Mutant P1 group	Mutant P2 group	P-value
Age	65.3 ± 9.9	67.6 ± 7.1	64.3 ± 11.2	
Gender				0.003
Female	234 (57.2)	12 (46.2)	22 (34.9)	
Male	175 (42.8)	14 (53.8)	41 (65.1)	
Pathological Stage				0.233*
Stage I	226 (55.3)	14 (53.8)	30 (47.6)	
Stage II	99 (24.2)	5 (19.2)	17 (27.0)	
Stage III	67 (16.4)	5 (19.2)	9 (14.3)	
Stage IV	15 (3.7)	2 (7.7)	7 (11.1)	
Unknown	2 (0.5)	0 (0)	0 (0)	
Smoking Status				0.033*
Non-smoker	66 (16.1)	1 (3.8)	5 (7.9)	
Current smoker	96 (23.5)	5 (19.2)	16 (25.4)	
Reformed smoker (> 15 years)	105 (25.7)	12 (46.2)	11 (17.5)	
Reformed smoker (≤ 15 years)	127 (31.1)	8 (30.8)	28 (44.4)	
Unknown	15 (3.7)	0 (0)	3 (4.8)	
* Samples with unknown information were removed when comparisons were conducted among groups.				

### Basic biological features of *KEAP1/NFE2L2*-mutant subtypes

GSEA was performed in *KEAP1/NFE2L2*-mutant subtypes in both patients and cell line cohorts. As shown in Fig. 3A and 3B, P2 and C2 subtypes were both enriched in pathways, such as *KRAS* signaling, *IL2/STAT5* signaling, apoptosis, and interferon alpha and gamma response. GSEA showed similarities between P2 and C2 subtypes, validating the integration and clustering to some degree.

Moreover, both P2 and C2 subtypes were associated with regulations of immune-related pathways, such as activations of T cells and macrophages (Supplement Fig. 1A and 1B). The results revealed that P2 and C2 subgroups displayed active immune pathways compared with P1 and C1 subgroups.

The P2 subgroup was found associated with higher proportions of *TP53* ( $P < 0.001$ ), *PCLO* ( $P = 0.011$ ), *NF1* ( $P = 0.029$ ) and *PTPRT* ( $P = 0.040$ ) mutations, while the P1 subgroup may have more patients with *STK11* ( $P = 0.008$ ) mutation (Supplement Table 1). However, we did not validate the mutational associations in lung adenocarcinoma cell lines owing to the small sample size.

### **Immunological features of the KEAP1/NFE2L2-mutant subtypes**

The tumor-infiltrating lymphocyte fractions were compared according to Saltz et al stratified by the mutation status [28]. Compared with the wild-type samples, lung adenocarcinoma harboring *KEAP1/NFE2L2* had a significantly lower lymphocyte fractions ( $P = 0.001$ , Fig. 4A). Subgroup analyses revealed that the P2 group exhibited significantly higher lymphocyte fractions compared with the P1 group ( $P < 0.001$ , Fig. 4A). We also observed that significant differences of ESTIMATE scores exist among three groups, in which P1 was linked to the lowest score (Fig. 4B, 4C and 4D). Based on TIMER, a significant decrease was found in the infiltrating levels of CD4 + T cells ( $P < 0.001$ ), CD8 + T cells ( $P = 0.011$ ), B cells ( $P < 0.001$ ), neutrophils ( $P < 0.001$ ), dendritic cells ( $P < 0.001$ ), and macrophages ( $P = 0.008$ ) in the mutant subgroup. (Fig. 3B). Moreover, the P1 subgroup was associated with reduced infiltrations of B cells ( $P = 0.017$ ), CD4 + T cells ( $P = 0.001$ ), neutrophils ( $P = 0.002$ ) and dendritic cells ( $P = 0.006$ ) (Fig. 4E). Furthermore, P2 subtype was associated with higher number of immunogenic mutations than P1 group (Fig. 4F).

### **Smoking-related genomic features of the KEAP1/NFE2L2-mutant subtypes of lung adenocarcinoma**

First, the methylation levels were compared across mutant subgroups. 84,700 and 64,204 differentially hypermethylated probes were found in the P1 and P2 groups, respectively (Fig. 5A). Meanwhile, 8,981 hypermethylated probes were found in the C1 group, while 5,933 hypermethylated probes were found in the C2 group (Fig. 5B). Next, unique smoking-related probes were extracted according to Vaz et al [31]. Both P2 and C2 groups displayed a similar trend of hypermethylation compared with the P1 and C1 groups (Fig. 5C-D). The results suggested that smoking-related epigenomic alterations might play essential roles in *KEAP1/NFE2L2*-mutant subgroups. The epigenomic similarities also confirmed a potential resemblance between patient and cell line mutant subsets.

Second, we assessed the somatic mutational patterns of all lung adenocarcinoma patients and obtained four distinctive signatures (Supplement Fig. 2A). Among them, signature 2 subgroup (W2) was highly similar to Signature 4 and 29 of thirty known somatic mutational signatures in the COSMIC database, which were closely associated with smoking and tobacco chewing (coefficient of cosine similarity = 0.805 and 0.740). Then, we compared the normalized activities of the identified W2 mutational signature between *KEAP1/NFE2L2*-mutant subgroups. We found that P2 subset had significantly higher activities of W2 signature than P1 subset (Supplement Fig. 2B,  $P = 0.004$ ), which further indicated possible different roles of smoking in the mutant subgroups.

### **Screening for compounds with potential sensitivity to the KEAP1/NFE2L2-mutant subtypes**

After characterizing the clinical and biological features of the mutant subtypes, possible cancer-associated drugs which were sensitive to each subtype were explored. More than 400 drugs or compounds were tested on *KEAP1/NFE2L2*-mutant or wild-type lung adenocarcinoma cell lines in GDSC. This study aimed to target cancer-associated drugs or compounds with potential specific sensitivity to C1 or C2. 38 drugs, which were potentially sensitive to the C2 *KEAP1/NFE2L2*-mutant subtype, were discovered (Supplement Table 2). Although the criteria were adjusted, only one C1-specific compound was identified (Supplement Table 2).

C2-specific drugs were found to be mainly composed of the following types. First, inhibitors of the *PI3K/Akt* signaling pathways, such as afuresertib, AZD8186 and AMG-319 might be sensitive to the C2 *KEAP1/NFE2L2*-mutant subgroup compared with the C1 and wild-type groups (Fig. 6 and Supplement Table 2). Second, inhibitors of *IGF1R* signaling, such as BMS-536924, linsitinib and NVP-ADW742, showed better efficacy in the C2 subset (Fig. 6 and Supplement Table 2). Moreover, drugs that target *Wnt* and *MAPK/Erk* signaling pathways were more toxic to the C2 group (Fig. 6 and Supplement Table 2). In addition, chemotherapy drugs, such as docetaxel, epothilone B and vinorelbine were found to preferentially kill the cells in the C2 subgroup (Fig. 6 and Supplement Table 2). Nevertheless, only one compound (EHT-1864) was found that might be sensitive to the C1 subset compared with C2 and wild-type cell lines (Fig. 6 and Supplement Table 2). The selected compound, EHT-1864, is an inhibitor of *Rac1*, *Rac2* and *Rac3* and mediated the reorganization of actin cytoskeleton.

## Discussion

The *KEAP1/NFE2L2* mutations were observed in many common malignant tumors, including lung adenocarcinoma [8, 9, 16, 18], which might define a molecular subset of rapidly progressing tumor [35]. In this study, the multiplatform data from TCGA were adopted to identify subsets of lung adenocarcinoma with *KEAP1/NFE2L2* mutations. Clinicopathological and bioinformatics analyses, such as immune microenvironment and methylation level, were performed to further explore the intrinsic heterogeneities of *KEAP1/NFE2L2*-mutant disease. Moreover, cell line samples were used for drug sensitivity screening based on public datasets. In addition, *CUL3* mutation was not included as the genomic signature in this study. *CUL3* belonged to the ubiquitin-proteasome system, which was involved in many oncogenic processes, and could not be considered as a specific *KEAP1/NFE2L2* pathway component [36].

Variations in the *KEAP1-NFE2L2* pathway were detected in more than 20% patients with lung cancer, which represented one of the major molecular subtypes [8, 9]. Goeman et al revealed that *KEAP1/NFE2L2* mutations represented a negative factor of survival, which defined a rapidly progressing molecular subtype [35, 37]. The mutant type showed heterogeneities, and one subset was associated with significantly worse survival. Cai et al performed a similar study and divided *KEAP1/NFE2L2*-mutant lung adenocarcinoma into three subsets based on gene profiling. The present study integrated multi-omics datasets, such as somatic mutation, methylation, and miRNA, to cluster into two subsets. P2/C2 subset displayed active immune pathways compared with the P1/C1 subgroups. Clinical features, somatic mutation signatures and methylation levels showed potential associations with patients' smoking history.

Previous studies demonstrated that smoking led to significant nuclear translocation of *NFE2L2*, which might be potentially fatal in smoking-related lung tumorigenesis [38, 39]. Moreover, aberrant *KEAP1/NFE2L2* functions could also be an advantageous strategy of the tumor to protect itself against oxidative stress [39]. These findings might also be potential evidence of distinct *KEAP1/NFE2L2* subtypes.

Furthermore, drug sensitivities of cell lines from public datasets were analyzed and several subgroup-specific drugs were discovered in our study. Best et al observed that synergy between *KEAP1/NFE2L2* and *PI3K* pathways promoted lung cancer progression with the altered immune milieu, which supported the compound screening results of inhibitors of *PI3K/Akt* pathways in this study [10]. Several studies revealed possible associations between the two pathways [40, 41]. The pathway analyses of this study also revealed that *PI3K/Akt* pathway was enriched in the P2 subgroup. Vartanian et al identified alternative pathways critical for *NFE2L2*-dependent growth in *KEAP1*-mutant cell lines, including *IGF1R* [33]. The findings in this study suggested that inhibitors of *IGF1R* signaling were effective in the C2 subtype. Only one alternative compound existed, which inhibited *Rac* signaling to mediate the actin cytoskeleton. Wu et al demonstrated that *KEAP1* stabilized F-actin cytoskeleton structures and inhibited focal adhesion, thereby restraining migrations and invasions of lung cancers [34]. *KEAP1/NFE2L2/CUL3* represented a mechanism of resistance to tyrosine kinase inhibitor in patients with *EGFR*-mutant non-small cell lung cancer [19]. Most identified compounds in our study were sensitive to the C2 subgroup which represented a subset with a worse prognosis. However, only one compound showed better efficacy to the C1 group with a revised statistical threshold, revealing difficulties in selecting appropriate drugs. However, the intrinsic differences in immune infiltrations suggested distinct immunotherapy strategies, especially developing drugs for the C2/P2 group. Also, concurrent alterations, like *STK11* and *TP53*, could also be potential targets in *KEAP1/NFE2L2*-mutant diseases.

There were also limitations that should be mentioned in this study. First, it had a small sample size of mutant cell lines and patients. The study explored intrinsic heterogeneities of *KEAP1/NFE2L2*-mutant lung adenocarcinoma. However, further studies are required to better characterize and precisely differentiate each mutant subtype. Although LN(IC50) was adopted from GDSC to measure compound sensitivities, more experiments should be conducted to test drug efficacy.

## Conclusion

Two subtypes of *KEAP1/NFE2L2*-mutant lung adenocarcinoma were identified based on both patient and cell line samples, and genomic and clinicopathological features of *KEAP1/NFE2L2* mutations were characterized. The intrinsic heterogeneities of *KEAP1/NFE2L2* mutations was found to be associated with immune microenvironment and smoking-related genomic aberrations.

## Declarations

### Ethics approval and consent to participate

Not applicable.

### **Consent for publication**

Not applicable.

### **Availability of data and materials**

All data could be downloaded from public databases (TCGA, GEO, CCLE, GDSC and XENA databases) and previous literatures in the reference. The datasets used and/or analyzed during the current study available from the corresponding author on reasonable request.

### **Competing interests**

None.

### **Funding**

This work was supported by: The National Natural Science Foundation of China (81970092) and The Research and Development Fund of Zhongshan Hospital, Fudan University (2019ZSFZ19 and 2018ZSFZ002).

### **Authors' contributions**

(I) Conception and design: XD Y; M L; ZC C; C Z

(II) Administrative support: Q W; L W; C Z

(III) Provision of study materials or patients: XD Y; M L; ZC C; L G; B J; YW H

(IV) Collection and assembly of data: XD Y; M L; ZC C

(V) Data analysis and interpretation: XD Y; M L; ZC C; L G; B J; YW H

(VI) Manuscript writing: All authors.

(VII) Final approval of manuscript: All authors

### **Acknowledgements**

We would like to thank International Science Editing Co. for language editing service of this manuscript.

## **References**

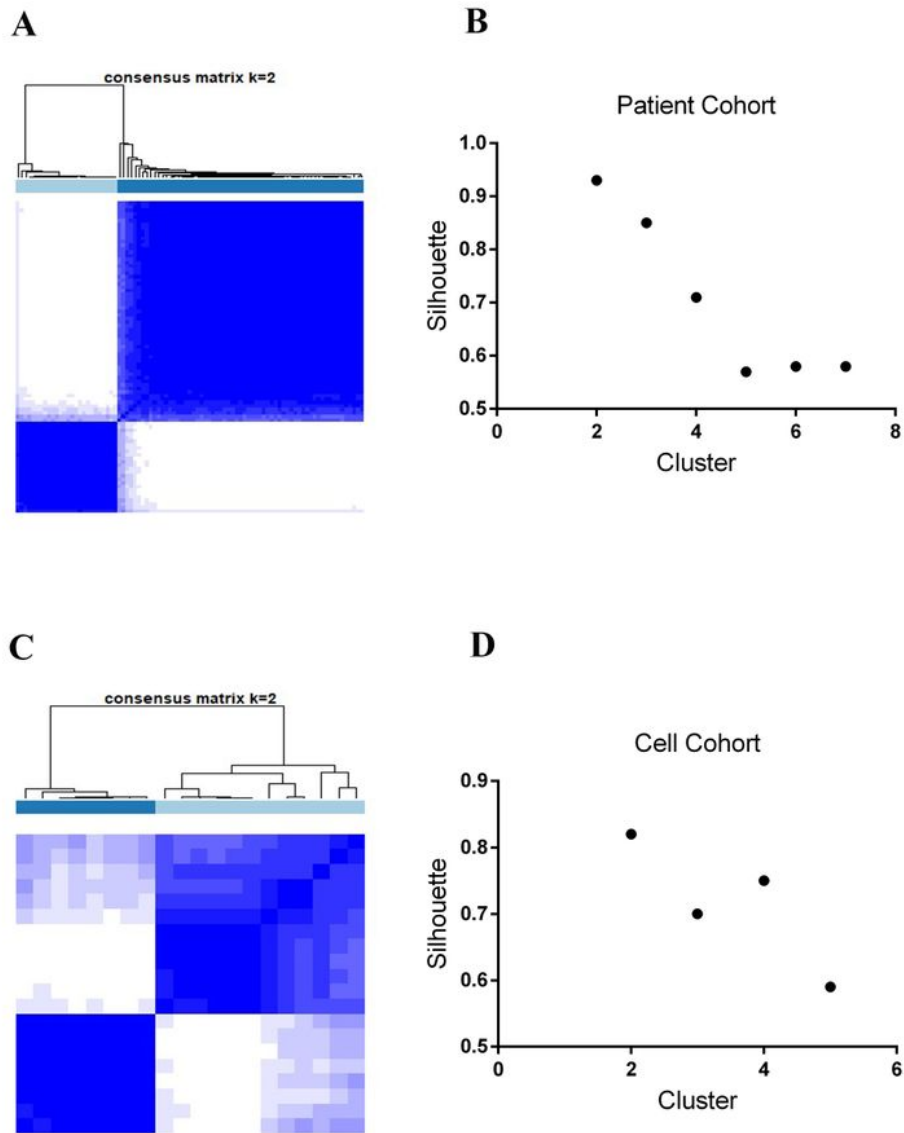
1. Siegel RL, Miller KD, Jemal A: Cancer statistics, 2019. CA Cancer J Clin 2019;69:7–34.

2. Bray F, Ferlay J, Soerjomataram I, et al.: Global cancer statistics 2018: GLOBOCAN estimates of incidence and mortality worldwide for 36 cancers in 185 countries. *CA Cancer J Clin* 2018;68:394–424.
3. Lu T, Yang X, Huang Y, et al.: Trends in the incidence, treatment, and survival of patients with lung cancer in the last four decades. *Cancer Manag Res* 2019;11:943–953.
4. Siegel RL, Miller KD, Jemal A: Cancer statistics, 2020. *CA Cancer J Clin* 2020;70:7–30.
5. Sato M, Shames DS, Gazdar AF, Minna JD: A translational view of the molecular pathogenesis of lung cancer. *J Thorac Oncol* 2007;2:327–343.
6. Lynch TJ, Bell DW, Sordella R, et al.: Activating mutations in the epidermal growth factor receptor underlying responsiveness of non-small-cell lung cancer to gefitinib. *N Engl J Med* 2004;350:2129–2139.
7. Shaw AT, Engelman JA: ALK in lung cancer: past, present, and future. *J Clin Oncol* 2013;31:1105–1111.
8. Comprehensive genomic characterization of squamous cell lung cancers. *Nature* 2012;489:519–525.
9. Comprehensive molecular profiling of lung adenocarcinoma. *Nature* 2014;511:543–550.
10. Best SA, De Souza DP, Kersbergen A, et al.: Synergy between the KEAP1/NRF2 and PI3K Pathways Drives Non-Small-Cell Lung Cancer with an Altered Immune Microenvironment. *Cell Metab* 2018;27:935–943.
11. Romero R, Sayin VI, Davidson SM, et al.: Keap1 loss promotes Kras-driven lung cancer and results in dependence on glutaminolysis. *Nat Med* 2017;23:1362–1368.
12. Solis LM, Behrens C, Dong W, et al.: Nrf2 and Keap1 abnormalities in non-small cell lung carcinoma and association with clinicopathologic features. *Clin Cancer Res* 2010;16:3743–3753.
13. Holmstrom KM, Finkel T: Cellular mechanisms and physiological consequences of redox-dependent signalling. *Nat Rev Mol Cell Biol* 2014;15:411–421.
14. Tian Y, Liu Q, He X, et al.: Emerging roles of Nrf2 signal in non-small cell lung cancer. *J Hematol Oncol* 2016;9:14.
15. Best SA, Sutherland KD: "Keeping" a lid on lung cancer: the Keap1-Nrf2 pathway. *Cell Cycle* 2018;17:1696–1707.
16. Gao YB, Chen ZL, Li JG, et al.: Genetic landscape of esophageal squamous cell carcinoma. *Nat Genet* 2014;46:1097–1102.
17. Singh A, Misra V, Thimmulappa RK, et al.: Dysfunctional KEAP1-NRF2 interaction in non-small-cell lung cancer. *PLoS Med* 2006;3:e420.
18. Guichard C, Amaddeo G, Imbeaud S, et al.: Integrated analysis of somatic mutations and focal copy-number changes identifies key genes and pathways in hepatocellular carcinoma. *Nat Genet* 2012;44:694–698.
19. Hellyer JA, Stehr H, Das M, et al.: Impact of KEAP1/NFE2L2/CUL3 mutations on duration of response to EGFR tyrosine kinase inhibitors in EGFR mutated non-small cell lung cancer. *Lung Cancer*

- 2019;134:42–45.
20. Jeong Y, Hellyer JA, Stehr H, et al.: Role of KEAP1/NFE2L2 Mutations in the Chemotherapeutic Response of Patients with Non-Small Cell Lung Cancer. *Clin Cancer Res* 2020;26:274–281.
  21. Frank R, Scheffler M, Merkelbach-Bruse S, et al.: Clinical and Pathological Characteristics of KEAP1- and NFE2L2-Mutated Non-Small Cell Lung Carcinoma (NSCLC). *Clin Cancer Res* 2018;24:3087–3096.
  22. Ellrott K, Bailey MH, Saksena G, et al.: Scalable Open Science Approach for Mutation Calling of Tumor Exomes Using Multiple Genomic Pipelines. *Cell Syst* 2018;6:271–281.
  23. Bairoch A: The Cellosaurus, a Cell-Line Knowledge Resource. *J Biomol Tech* 2018;29:25–38.
  24. Robin T, Capes-Davis A, Bairoch A: CLASTR: The Cellosaurus STR similarity search tool - A precious help for cell line authentication. *Int J Cancer* 2019.
  25. Chen YA, Lemire M, Choufani S, et al.: Discovery of cross-reactive probes and polymorphic CpGs in the Illumina Infinium HumanMethylation450 microarray. *Epigenetics* 2013;8:203–209.
  26. Wilkerson MD, Hayes DN: ConsensusClusterPlus: a class discovery tool with confidence assessments and item tracking. *Bioinformatics* 2010;26:1572–1573.
  27. Hanzelmann S, Castelo R, Guinney J: GSVA: gene set variation analysis for microarray and RNA-seq data. *BMC Bioinformatics* 2013;14:7.
  28. Saltz J, Gupta R, Hou L, et al.: Spatial Organization and Molecular Correlation of Tumor-Infiltrating Lymphocytes Using Deep Learning on Pathology Images. *Cell Rep* 2018;23:181–193.
  29. Yoshihara K, Shahmoradgoli M, Martinez E, et al.: Inferring tumour purity and stromal and immune cell admixture from expression data. *Nat Commun* 2013;4:2612.
  30. Li B, Severson E, Pignon JC, et al.: Comprehensive analyses of tumor immunity: implications for cancer immunotherapy. *Genome Biol* 2016;17:174.
  31. Vaz M, Hwang SY, Kagiampakis I, et al.: Chronic Cigarette Smoke-Induced Epigenomic Changes Precede Sensitization of Bronchial Epithelial Cells to Single-Step Transformation by KRAS Mutations. *Cancer Cell* 2017;32:360–376.
  32. Kim J, Mouw KW, Polak P, et al.: Somatic ERCC2 mutations are associated with a distinct genomic signature in urothelial tumors. *Nat Genet* 2016;48:600–606.
  33. Vartanian S, Lee J, Klijn C, et al.: ERBB3 and IGF1R Signaling Are Required for Nrf2-Dependent Growth in KEAP1-Mutant Lung Cancer. *Cancer Res* 2019;79:4828–4839.
  34. Wu B, Yang S, Sun H, et al.: Keap1 Inhibits Metastatic Properties of NSCLC Cells by Stabilizing Architectures of F-Actin and Focal Adhesions. *Mol Cancer Res* 2018;16:508–516.
  35. Goeman F, De Nicola F, Scalera S, et al.: Mutations in the KEAP1-NFE2L2 Pathway Define a Molecular Subset of Rapidly Progressing Lung Adenocarcinoma. *J Thorac Oncol* 2019;14:1924–1934.
  36. Scott DC, Rhee DY, Duda DM, et al.: Two Distinct Types of E3 Ligases Work in Unison to Regulate Substrate Ubiquitylation. *Cell* 2016;166:1198–1214.

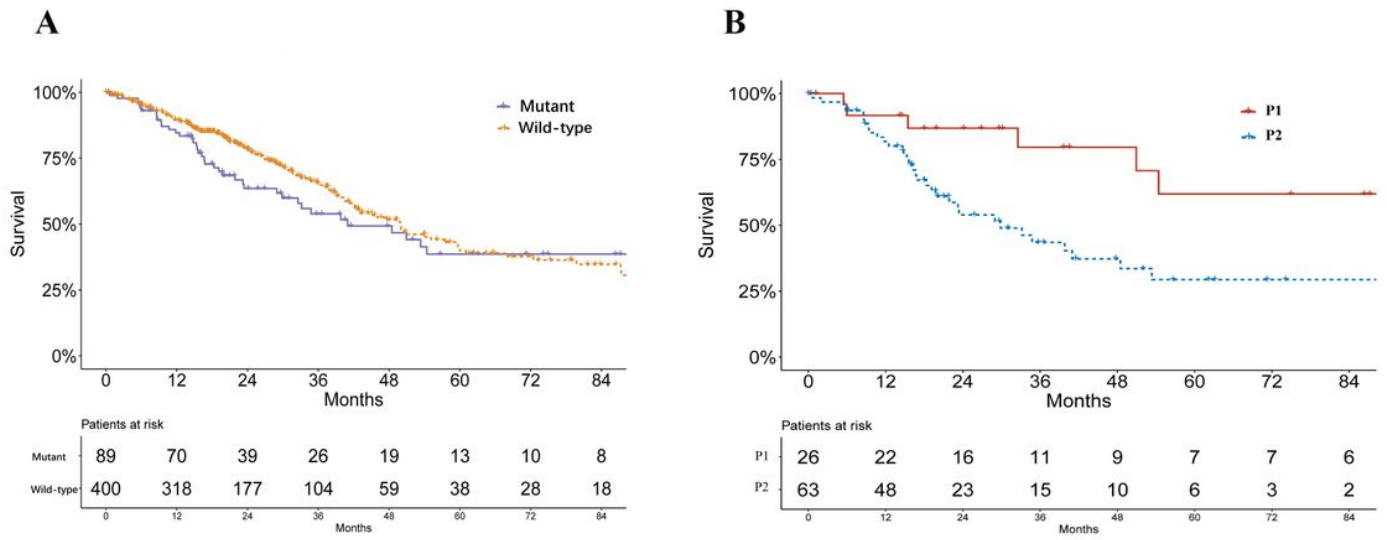
37. Takahashi T, Sonobe M, Menju T, et al.: Mutations in Keap1 are a potential prognostic factor in resected non-small cell lung cancer. *J Surg Oncol* 2010;101:500–506.
38. Chang WH, Thai P, Xu J, et al.: Cigarette Smoke Regulates the Competitive Interactions between NRF2 and BACH1 for Heme Oxygenase-1 Induction. *Int J Mol Sci* 2017;18.
39. Muller T, Hengstermann A: Nrf2: friend and foe in preventing cigarette smoking-dependent lung disease. *Chem Res Toxicol* 2012;25:1805–1824.
40. Kaufman JM, Amann JM, Park K, et al.: LKB1 Loss induces characteristic patterns of gene expression in human tumors associated with NRF2 activation and attenuation of PI3K-AKT. *J Thorac Oncol* 2014;9:794–804.
41. Dai B, Yoo SY, Bartholomeusz G, et al.: KEAP1-dependent synthetic lethality induced by AKT and TXNRD1 inhibitors in lung cancer. *Cancer Res* 2013;73:5532–5543.

## Figures



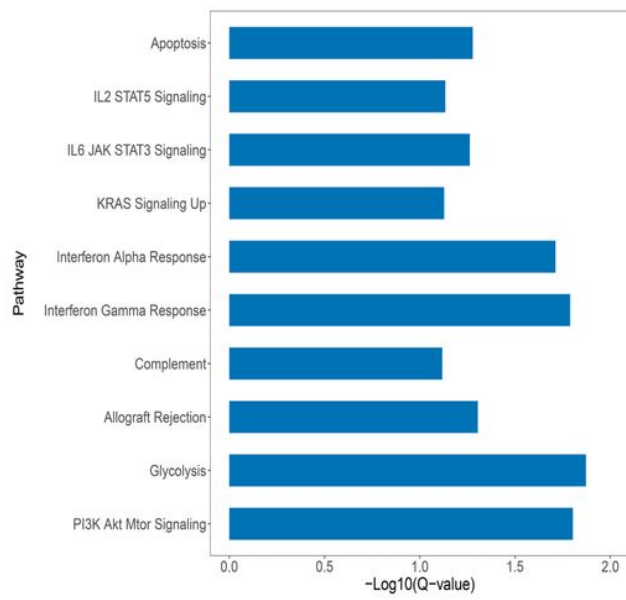
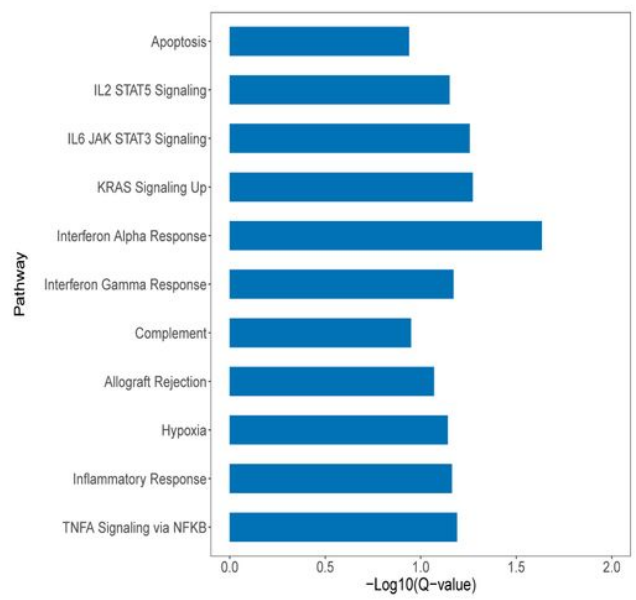
**Figure 1**

The SNF fused five types of datasets and consensus clustering identifies subsets of KEAP1/NFE2L2-mutant lung adenocarcinoma in patients and cell lines. A. Two subsets of KEAP1/NFE2L2-mutant patients were identified. B. Silhouette values of patient clustering with the  $k = 2$  to 7. C. Two subsets of KEAP1/NFE2L2-mutant cell lines were identified. D. Silhouette values of cell line clustering with the  $k = 2$  to 5.



**Figure 2**

Survival curves of lung adenocarcinoma patients in TCGA. A. Survival curves of KEAP1/NFE2L2 mutant and wild-type patients. (P = 0.212) B. Survival curves of KEAP1/NFE2L2 mutant patient subgroups (P1 and P2). (P = 0.020)

**A****B**

### Figure 3

A. The enriched pathways in Hallmark of KEAP1/NFE2L2 mutant P2 patient subgroup. B. The enriched pathways in Hallmark of KEAP1/NFE2L2 mutant C2 cell line subgroup.

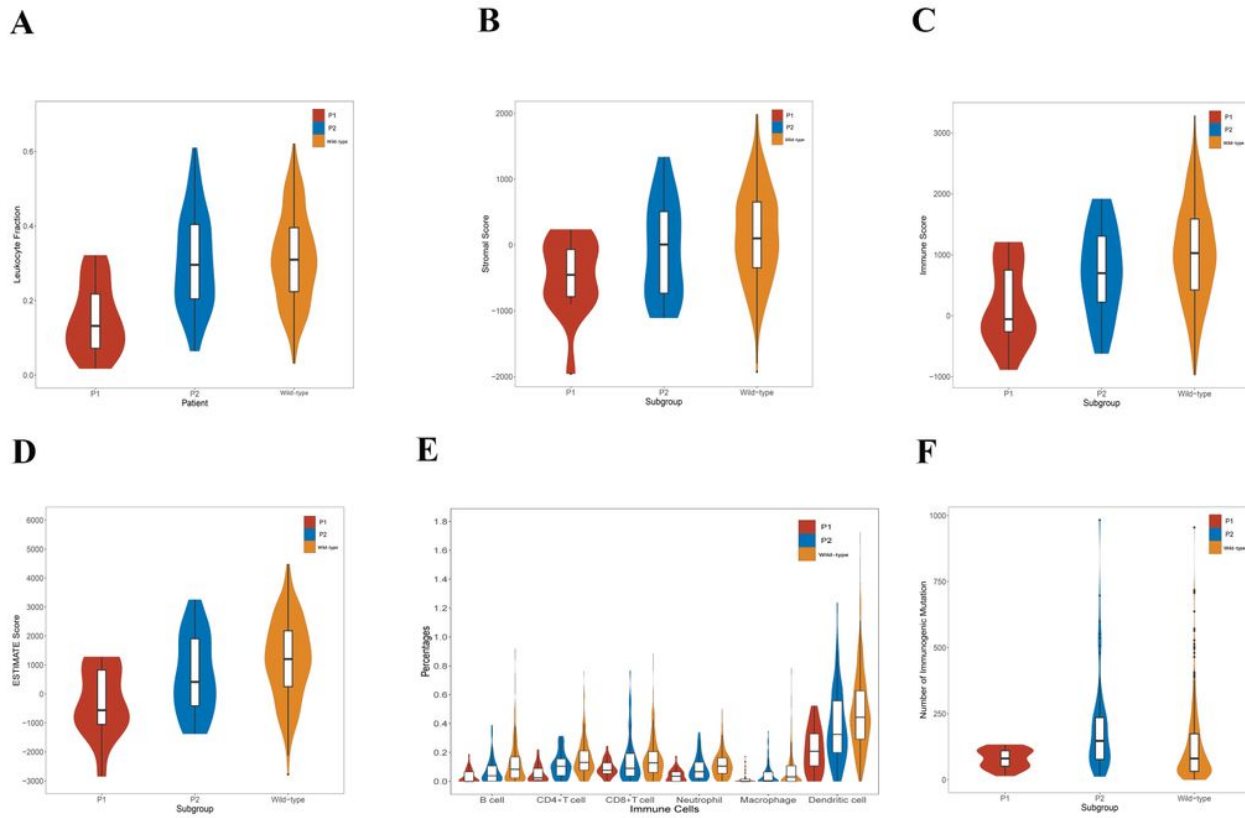


**Figure 4**

Immunological features of lung adenocarcinoma patients in TCGA. A. Comparison of leukocyte fraction stratified by KEAP1/NFE2L2 mutant (P1 and P2) and wild-type patient subgroups. (mutant group vs. wild-type group,  $P = 0.001$ ; P1 group vs. P2 group,  $P < 0.001$ ) B. Comparison of stromal score calculated by ESTIMATE algorithm stratified by KEAP1/NFE2L2 mutant (P1 and P2) and wild-type patient subgroups. (P1 vs. P2 vs. wild-type group,  $P = 0.005$ ) C. Comparison of immune score calculated by ESTIMATE algorithm stratified by KEAP1/NFE2L2 mutant (P1 and P2) and wild-type patient subgroups. (P1 vs. P2 vs. mutant group,  $P = 0.001$ ) D. Comparison of ESTIMATE score calculated by ESTIMATE algorithm stratified by KEAP1/NFE2L2 mutant. (P1 and P2) and wild-type patient subgroups. (P1 vs. P2 vs. wild-type group,  $P = 0.001$ ) E. Comparison of tumor-infiltrating immune cells stratified by KEAP1/NFE2L2 mutant (P1 and P2) and wild-type patient subgroups based on TIMER database. [mutant group vs. wild-type group: CD4+ T cells ( $P < 0.001$ ), CD8+ T cells ( $P = 0.011$ ), B cells ( $P < 0.001$ ), neutrophils ( $P < 0.001$ ), dendritic cells ( $P < 0.001$ ), and macrophages ( $P = 0.008$ ); P1 group vs. P2 group: B cells ( $P = 0.017$ ), CD4+ T cells ( $P = 0.001$ ), CD8+ T cells ( $P = 0.375$ ), neutrophils ( $P = 0.002$ ), macrophages ( $P = 0.113$ ), and dendritic cells ( $P = 0.006$ )] F. Comparison of the number of immunogenic mutations per sample stratified

by KEAP1/NFE2L2 mutant (P1 and P2) and wild-type patient subgroups. (P1 vs. P2 vs wild-type group,  $P < 0.001$ )

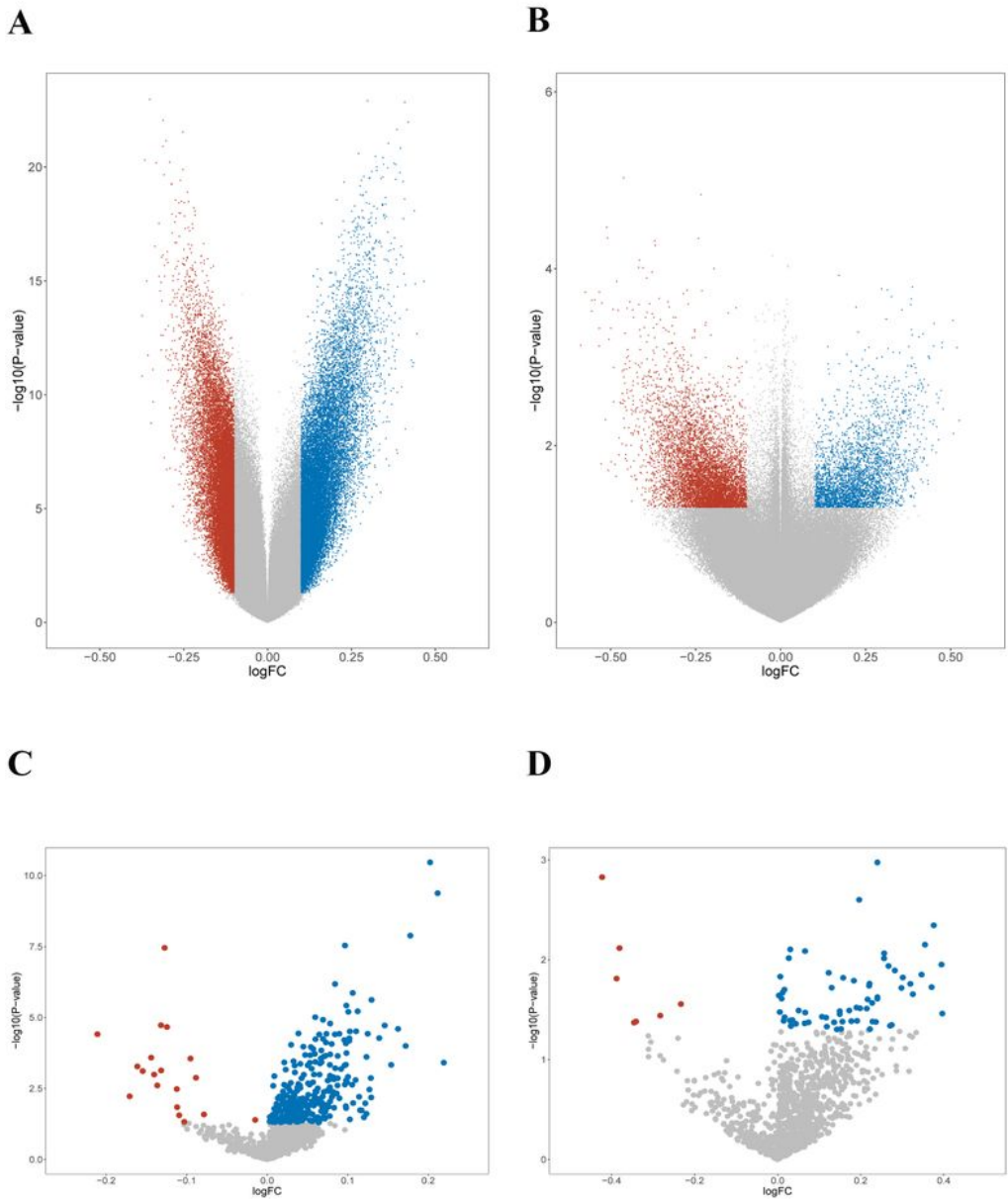


**Figure 5**

Epigenomic features of the lung adenocarcinoma KEAP1/NFE2L2 mutant subgroups in patients and cell lines. A. Volcano plot of the global DNA methylation difference between patient mutant subgroups (P1 and P2). B. Volcano plot of the global DNA methylation difference between cell line mutant subgroups

(C1 and C2). C. Volcano plot of the smoking-related methylation signatures between patient mutant subgroups (P1 and P2). D. Volcano plot of the smoking-related methylation signatures between cell line mutant subgroups (C1 and C2).

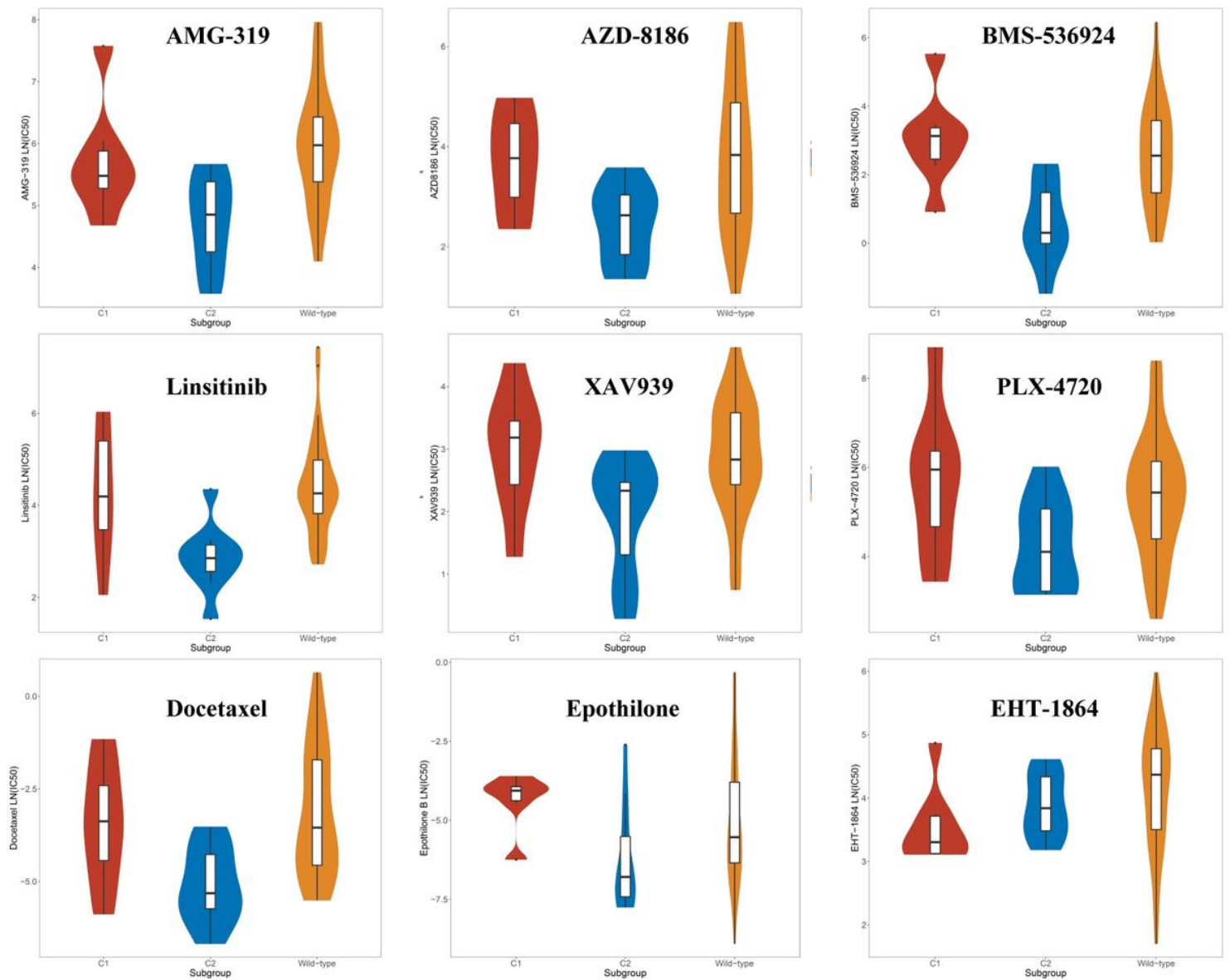


**Figure 6**

Screened drugs with selective sensitivity toward the KEAP1/NFE2L2-mutant subtypes

## Supplementary Files

This is a list of supplementary files associated with this preprint. Click to download.

- [SupplementFigure1.jpg](#)
- [SupplementFigure2.jpg](#)
- [SupplementTable1.docx](#)

- [SupplementTable2.docx](#)
- [supplementaryinformation.docx](#)